Journal of Atmospheric and Solar-Terrestrial Physics 167 (2018) 58–65

Contents lists available at ScienceDirect

Journal of Atmospheric and Solar-Terrestrial Physics

journal homepage: www.elsevier.com/locate/jastp

# Influence of air parcel trajectories on $CO_2$ and $CH_4$ concentrations in the northern plateau of the Iberian Peninsula

Isidro A. Pérez *, M. Luisa Sánchez, M. Ángeles García, Nuria Pardo

*Department of Applied Physics, Faculty of Sciences, University of Valladolid, Paseo de Belén, 7, 47011 Valladolid, Spain*

ARTICLE INFO

*Keywords:*
METEX
South-western Europe
Carbon dioxide
Methane

ABSTRACT

This study presents a simpler procedure for grouping air parcel back trajectories than others previously applied. Two-day air parcel back trajectories reaching an unpolluted site in the centre of the northern plateau of the Iberian Peninsula were calculated over a three-year period using the METEX model. A procedure based on the kernel density calculation was applied to the direction of each trajectory centroid to determine groups of trajectories. This method is much faster than the cluster procedure when it comes to retaining the directional details of groups. Seasonal analysis of six groups of trajectories revealed that the Atlantic origin prevailed against displacement from northern Europe. Moreover, Mediterranean and particularly African trajectories were infrequent, probably due to the rough peninsular orography in these directions. The location of air trajectories reaching the study site was described using a surface classification below the air parcels with improved spatial resolution compared to previous analyses. Local contribution was very marked, particularly in summer. Mean trajectories were calculated for each group together with meteorological features and $CO_2$ and $CH_4$ concentrations. Groups may be identified by their mean temperature, wind speed, elevation and distance values. However, only two groups should be considered when analysing the two trace gases, one for trajectories from the Atlantic Ocean and the second for trajectories from the continent. Contrasts of about 4 ppm for $CO_2$ in summer and 0.023 ppm for $CH_4$ in winter were observed, revealing that air trajectories from the Atlantic Ocean were cleaner than those arriving from the continent. These differences were attributed to higher air stagnation over land.

## 1. Introduction

The goal of this study is to propose a procedure for grouping air parcel trajectories that can overcome the drawbacks associated to previous methods. Research focusing exclusively on air parcel trajectories is not common, since analysing them normally involves other elements, water vapour, chemicals or microorganisms, which is the aim of the present research. This study prioritizes trajectory analysis and uses $CO_2$ and $CH_4$, both trace gases at unpolluted sites, to investigate the relationship among air parcel trajectories and their concentrations.

When a high number of air parcel trajectories is considered, one problem is how to manage them. Statistical processing is necessary in order to ascertain the underlying behaviour. Several methods, such as potential source contribution function or trajectory sector analysis (Li et al., 2012), have been described in previous studies. Cluster analysis is a procedure used to separate data into groups that are not known a priori (Wilks, 2011), and is frequently employed in atmospheric research to replace the vast amount of data handled by a small number of groups whose features may easily be described. However, although this tool is widely used, certain disadvantages are unavoidable. Cape et al. (2000) presented an agglomerative and hierarchical algorithm that may be used with a low number of air parcel trajectories to guarantee a reasonable calculation time. However, a seed is required to begin the iterative procedure when the number of trajectories increases, as explained in Dorling et al. (1992). In this case, obtaining the final number of clusters remains slow when the number of trajectories is high.

Groups formed by the clustering method consider similar trajectories. Moreover, this is a mathematical, objective, procedure. The Euclidean metric, given by the square root of the addition of square distances between pairs of points corresponding at the same time in two trajectories, is frequently used (Coury and Dillner, 2007) although this metric does not distinguish distances between trajectories with different latitudes, but with similar longitudes. Moreover, since the final number of clusters must be low if it is to prove useful and interpretable, each group must perforce include trajectories with varied shapes and distances, such that forming groups with trajectories displaying similar features is

* Corresponding author.
*E-mail address:* iaperez@fa1.uva.es (I.A. Pérez).

https://doi.org/10.1016/j.jastp.2017.10.015
Received 30 September 2016; Received in revised form 19 October 2017; Accepted 31 October 2017
Available online 9 November 2017

extremely difficult.

A further drawback of the clustering technique concerns the rule determining the suitable number of clusters. Although numerical procedures have frequently been suggested (Kassomenos et al., 2010; Notaro et al., 2013), practical considerations, such as the explanation of the results, are imposed.

These disadvantages suggest the need to find an alternative procedure for grouping air parcel trajectories so as to shorten calculation time whilst retaining a substantial amount of information. This study is divided into two parts. The first presents and applies such a procedure. A seasonal study is conducted to show the yearly evolution. The second part of this research addresses the relationship between air parcel trajectory groups and $CO_2$ and $CH_4$, a subject under examination. Fang et al. (2016a) explored the influence of transport on both trace gases in concentrations recorded at the Shangdianzi regional background station, China, and highlighted two contrasting regions. Similarly, transport was considered at the Shangri-La station, in the remote southwest of China, which is influenced by northern Africa and south-western Asia (Fang et al., 2016b). Another example is presented by Buchholz et al. (2016), who studied source and meteorological influences on air quality in the city of Wollongong, Australia. Ozone production was associated with anticyclones on the east coast. However, ozone depletion was associated with continental transport or fast trajectories from southern latitudes. Tiwari et al. (2014) examined the role of monsoons on atmospheric $CO_2$ at two sites in western India and considered the influence of orography on air parcels. This study, therefore, investigates the influence of meteorology on concentrations of the two trace gases, whose behaviour has previously been described at the same site (Pérez et al., 2013, 2014).

## 2. Materials and methods

### 2.1. Experimental description

Measurements were obtained at the Low Atmosphere Research Centre (CIBA) (41° 48′ 50.25″ N, 4° 55′ 58.56″ W, 850 m a.s.l.), located in the centre of the northern plateau of the Iberian Peninsula, Fig. 1. Grass is the main vegetation at the site, which is surrounded by non-irrigated crops. The northern plateau covers just over 94,000 $km^2$ and is bounded by three mountain ranges with peaks exceeding 2000 m a.s.l. The Cantabrian Range lies to the north, and stretches nearly 500 km in length and 100 km in width, extending latitudinally. The Central System to the south stretches some 600 km in length and 30 km in width from west to east in its first part, then turning northeast in the rest. The plateau is also bounded to the east by the Iberian System, which extends northwest to southeast, with a length of about 500 km and a width of around 100 km. Only the west part of the plateau is not bounded by mountain ranges and open to airflow.

The campaign extended over three years and commenced on October 15, 2010. $CO_2$ and $CH_4$ dry concentrations were obtained at 8.3 m from soil surface using a Picarro G1301 analyser. Mahesh et al. (2015) highlight the calibrations in order to have precise and accurate measurements. These calibrations were performed every two weeks with using NOAA standards: 452.56, 399.27 and 348.55 ppm for $CO_2$ and 1.9904, 1.8420 and 1.6310 ppm for $CH_4$, which are values above, similar to, and below ambient concentrations, respectively. Calibration injection lasted five minutes for each gas. Graphical representation of concentration vs. time showed three plateaus, where periods of stable measurements were selected for comparison with the corresponding standard. Differences between averages of measured values and standards against these standards are around −0.30% for $CO_2$ and between −0.05 and 0.07% for $CH_4$. The following linear equations were based on the comparison between NOAA standards and measurements provided by the device in calibrations, and used to slightly correct the semi-hourly averages of the values recorded:

$$CO_{2\,C} = 1.00369\ CO_2 - 0.22882, \quad (1)$$

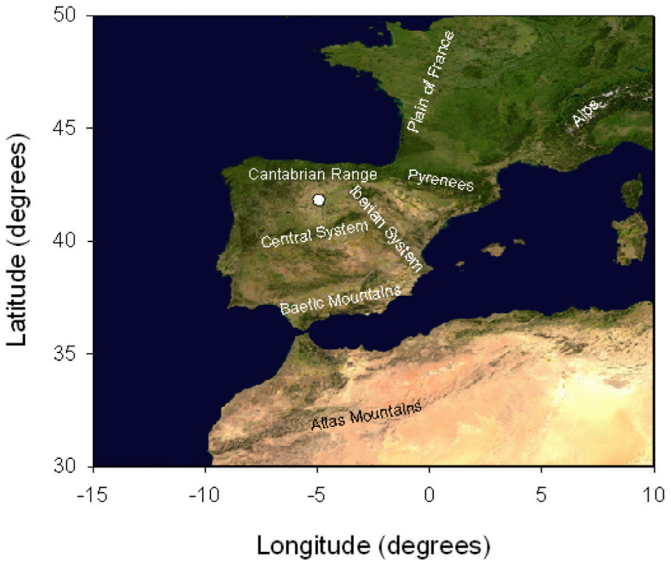


**Fig. 1.** NASA image where the site (white dot) and the main orographic features of the region are shown.

$$CH_{4\,C} = 0.99321\ CH_4 + 0.01206, \quad (2)$$

where the corrected value is marked by the subscript *C*.

Air parcel trajectory data, together with meteorological variables from two days prior to arrival at the study site, were obtained from the METEX model (Zeng et al., 2010). In this study, trajectories were calculated every hour and lasted 48 h. Moreover, the kinematic model where the trajectory is obtained with the horizontal wind components and the vertical pressure velocity was selected. Back trajectories were used to examine the airflow reaching the study site at 858 m a.s.l., which was the measurement height of trace gases. The results of the model are the date, coordinates and height above sea level of each trajectory point, boundary layer height, wind velocity components, temperature, potential temperature and pressure.

Since trajectories were provided every hour and comprised 49 points (one point each hour), concentrations were averaged every hour so as to make all of the data compatible.

### 2.2. Grouping trajectories

First, each trajectory provided by the METEX model was replaced by its corresponding centroid, which was calculated by averaging the longitude and latitude coordinates of the points that made up the trajectory. The centroid direction $\theta_i$, Fig. 2(a), was then calculated with the aid of the arrival point A (longitude $\lambda_0$ and latitude $\phi_0$) and the trajectory centroid B (longitude $\lambda$ and latitude $\phi$). Distance $c$ between A and B may be obtained using the Sinnott equation (Snyder, 1987).

$$\sin(c/2) = \left\{sin^2[(\phi - \phi_0)/2] + \cos\phi_0 \cos\phi\ sin^2[(\lambda - \lambda_0)/2]\right\}^{1/2} \quad (3)$$

The centroid direction was obtained with an expression deduced from the law of cosines

$$\cos(90 - \phi) = \cos(90 - \phi_0)\cos c + \sin(90 - \phi_0)\sin c \cos\theta_i, \quad (4)$$

where the argument of the trigonometric functions is expressed in degrees. When all of the centroid directions are calculated, the kernel method is used to estimate density, $f$, by

$$f(\theta) = (nh)^{-1} \sum_{i=1}^{n} K[(\theta - \theta_i)/h] \quad (5)$$

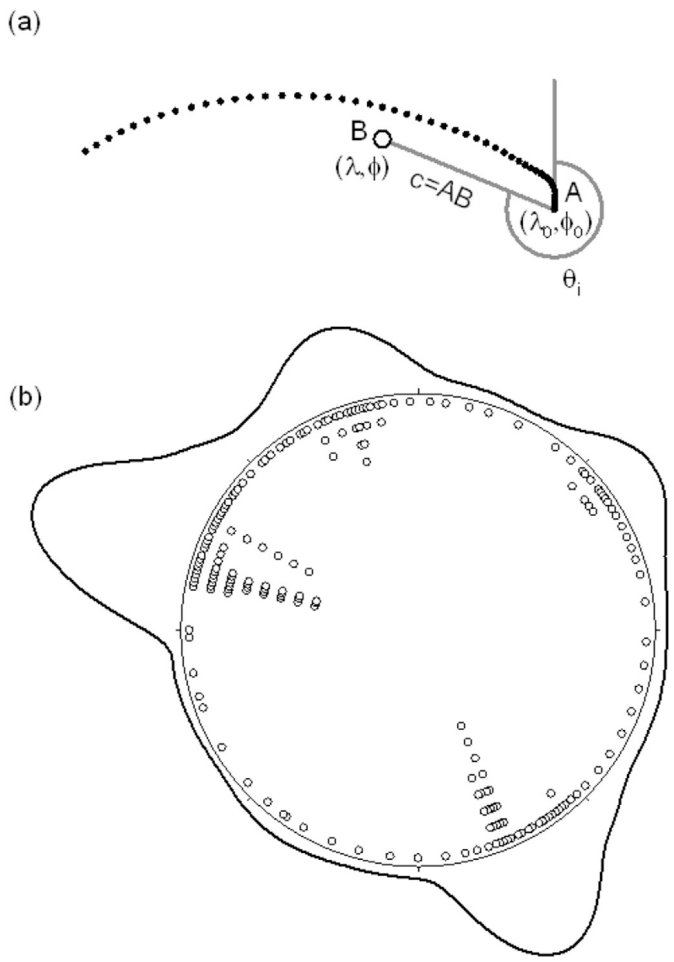


**Fig. 2.** Scheme showing (a) the trajectory points (black dots), arrival point (A), trajectory centroid (B), and its direction ($\theta_i$) and (b) centroids for different directions (white points) together with their density function (black line).

where $n$ is the number of trajectories, $h$ is a window width that controls the amount of smoothing and $\theta$ is the direction where the density is calculated. This study used the quartic kernel function considered by Fisher (1993).

$$K(x) = 0.9375\left(1 - x^2\right)^2 \quad -1 \le x \le 1. \tag{6}$$

Fig. 2(b) presents centroids with different directions together with their corresponding density, which is calculated using Eq. (5).

Once this density was calculated, minima of this function were determined and these formed the boundaries for the trajectory groups. The number of minima that should appear in the density function depends on each case and different values for $h$ must be considered in order to select a number of groups that is small enough to allow a simple representation of all of the trajectories, yet large enough to retain a sufficient amount of information. Consequently, the procedure presented emphasises direction, which is the first variable investigated in spatial analyses, and does not include the distance from the study site, assuming that it is extremely unlikely that different groups of air trajectories would be found in exactly the same direction.

### 2.3. Classification of air trajectories

This study follows Toledano et al. (2009), whose classification considers seven regions:

1) MP, maritime polar, corresponds to the Atlantic Ocean above 40° N,
2) MT, maritime tropical, for the Atlantic Ocean below 40° N,
3) A, maritime Arctic, for oceans above 60° N and land above the Arctic Circle,
4) C, continental, mainly Europe,
5) CT, continental tropical, for Africa,
6) Me, Mediterranean, for the Mediterranean Sea, and
7) L, local, for trajectory points within 2° of the study site.

The region considered in this study, located between 55° W-25° E and 20°-75° N, was represented by an image of 678 × 467 pixels, coloured in Fig. 3, following the classification previously described. With the aid of this representation, every point of each trajectory may be labelled with the corresponding sector of this figure.

## 3. Results

### 3.1. Air trajectories affecting the northern Iberian Peninsula

Different window widths have been considered following the procedure described in Section 2.2 to calculate the probability density function of the transport direction to the study site with a resolution of 1°. The cumulative value of the probability density function was equal to one for the full angular range. A window width of 20° was finally selected, which gave the six sectors shown in Fig. 4. This procedure is simpler and faster than the cluster method previously used at this site (Pérez et al., 2015).

Both angular widths and densities differed enormously for the sectors. However, narrow sectors were retained since they corresponded to prominent directions. Density values around or above 0.005 were observed for NNE-NE and NW in winter, W in spring and WNW-NW in summer, due to the extremely low values observed in other directions. However, autumn densities were lower, since the contrast between directions was smaller, although NNE and WNW showed maxima, and sector 2 extended from around S to around W.

Fig. 4 presents the directions of the groups formed. However, the spatial extent of trajectories belonging to each group may only be observed with a spaghetti plot, such as the one shown in Fig. 5 where seasonal frequencies were also indicated.

The main result of this representation is that zonal transport was more frequent than the meridional flow, with the westerly flow being more accentuated than the easterly flow, such as in group 5 in winter or group 4 in autumn (whose frequencies were 37.9 and 21.9% respectively). Air parcels from the north originated from greater distances compared to air

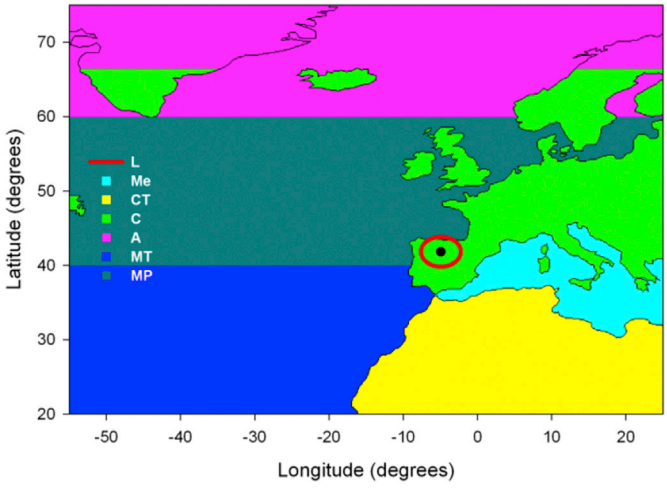


**Fig. 3.** Classification of air trajectories following their geographical position. Black point corresponds to the study site.

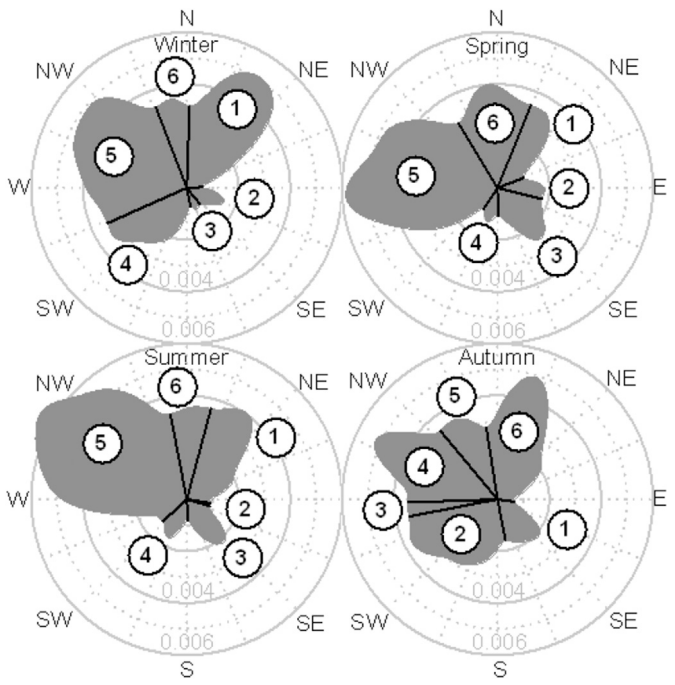


**Fig. 4.** Seasonal evolution of the angular density of centroid directions. Density minima are represented by black lines, and numbers in circles are labels for the angular sectors considered.

parcels from the south, and occasionally reached high latitudes, above 60°, such as groups 1 and 6 in winter or groups 5 and 6 in autumn.

A detailed description of the air features of these groups may be obtained by combining the coordinates of the trajectory points with the information presented in Fig. 3. The arrival point was not considered in this case so as not to overestimate local flow. Fig. 6 presents the result of this analysis. Local flow was frequent, particularly in summer (above 40% in most of the groups), although it was lower for groups 5 and 6 in winter and spring. Continental flow was also frequent (reaching 40% in some groups) and was attributed to the site location, in the centre on the northern plateau of the Iberian Peninsula. This flow was relatively low in autumn due to the long distances of its trajectories, since the maritime polar region featured prominently in this season (reaching around 60% in groups 4 and 5). Moreover, frequency of flow from this region was above 40% in groups 5 and 6 in the rest of the seasons. The remaining regions hardly appeared. This was the case of the maritime tropical region in group 4, which was noticeable in winter, and in groups 2 and 3 in autumn (between 20% and 35%). This was followed by the Mediterranean region, which appeared in some of the groups in all of the seasons. The Arctic region was present in one group in winter and in two groups in autumn, although with very low frequency. Finally, the continental tropical region was absent in spring and summer.

### 3.2. Influence of air trajectory on $CO_2$ and $CH_4$ concentrations

The availability of concentrations ranged from around 85% in summer to nearly 99% in spring. Mean seasonal values were calculated and presented in Table 1.

The means of $CO_2$ and $CH_4$ as chemical properties were calculated for each trajectory group, whose means of coordinates are presented in Fig. 7, together with some physical properties, mean temperature, wind speed, elevation above sea level and distance travelled.

Groups may be described by the mean values of temperature, wind speed, elevation and distance. Fisher's procedure of least significant differences was used to investigate whether groups may be considered separate and successfully formed when differences of pairs of mean values for every variable are statistically significant at a certain confidence level. A total of 15 differences were formed for the six groups in each season for every variable, giving 60 differences in the four seasons. All of the differences of mean temperature values were statistically significant at a 95% confidence level. Only one out of 15 differences was not significant in summer for wind speed. In the four seasons, three out of 60 differences were not significant for elevation, and six out of 60 differences for distances. Consequently, the groups formed were satisfactorily defined by the mean variables (temperature, wind speed, elevation and distance) provided by the trajectories.

Analysing each group's mean distance from the study site allowed intervals to be established so as to classify them according to their range (Markou and Kassomenos, 2010; Dimitriou and Kassomenos, 2013). The following intervals were proposed:

Short-range, 0 < distance <600 (km)
Medium-range, 600 < distance < 1 200 (km)
Long-range, 1 200 < distance < 1800 (km)
Very long-range, 1 800 < distance (km)

Groups within all of these ranges were present in winter, whereas ranges of groups in summer were mainly from short or medium distances. This latter range prevailed in spring groups, and groups were equally divided between medium and long range in autumn.

Quite different behaviour was observed for $CO_2$ and $CH_4$. When differences between average concentrations for each group and seasonal averages are calculated, greater values are only observed in infrequent directions. Positive differences for $CO_2$ are found for continental air trajectories in winter, although these differences are found for the southern direction in the remaining seasons together with the eastern direction in summer. For $CH_4$, positive differences are obtained in spring for the northern and southern directions, whereas such differences are found mainly for continental air trajectories in the remaining seasons.

Concentrations seemed to be linked with the type of surface, whether continental or maritime, from which the air approximately comes. Therefore, some groups were merged in order to obtain statistically significant mean differences following Fisher's least significant difference method. The results of this analysis are presented in Table 2. Concentration differences of merged groups with the average concentration in each season are not similar since observations are right-skewed. Concentrations of air trajectories from the ocean were lower than those for air trajectories linked to the continent. This behaviour is explained since air trajectories from the ocean were normally longer, and had a higher wind speed than continental air trajectories.

The greatest contrast for $CO_2$ between both groups of merged trajectories, 4.1 ppm, was observed in summer, a period when the lowest concentration for this gas was reached. Contrasting distances travelled by the air parcels justify this result. In this season, continental trajectories are limited to the Iberian Peninsula, revealing stagnation conditions, whereas oceanic trajectories are much longer. When separated groups are considered, this difference increased by up to nearly 7 ppm between group 2, with marked recirculation, and group 6, which travels mainly on the sea surface. No $CH_4$ contrast is observed in this period since concentrations linked to mean trajectories presented in Fig. 7 are similar, indicating that $CH_4$ concentration is independent of wind direction in summer. In fact, from Table 2 only the $CH_4$ concentration difference is not statistically significant in summer, revealing that the contrast between merged groups is given by other variables, such as direction or distance. The greatest contrast between the $CH_4$ concentrations of merged trajectories was observed in winter, 0.0230 ppm, when the mean concentration is the highest. This difference reaches 0.0388 ppm with separated groups 2 and 6. The trajectory for group 2 lies mainly on the ground with low wind speed, 4.1 m $s^{-1}$. However, for group 6, the air parcel travels mostly on the sea with high wind speed, 10.3 m $s^{-1}$.

This procedure thus revealed that oceanic air trajectories were cleaner than continental air trajectories, since stagnant conditions mainly

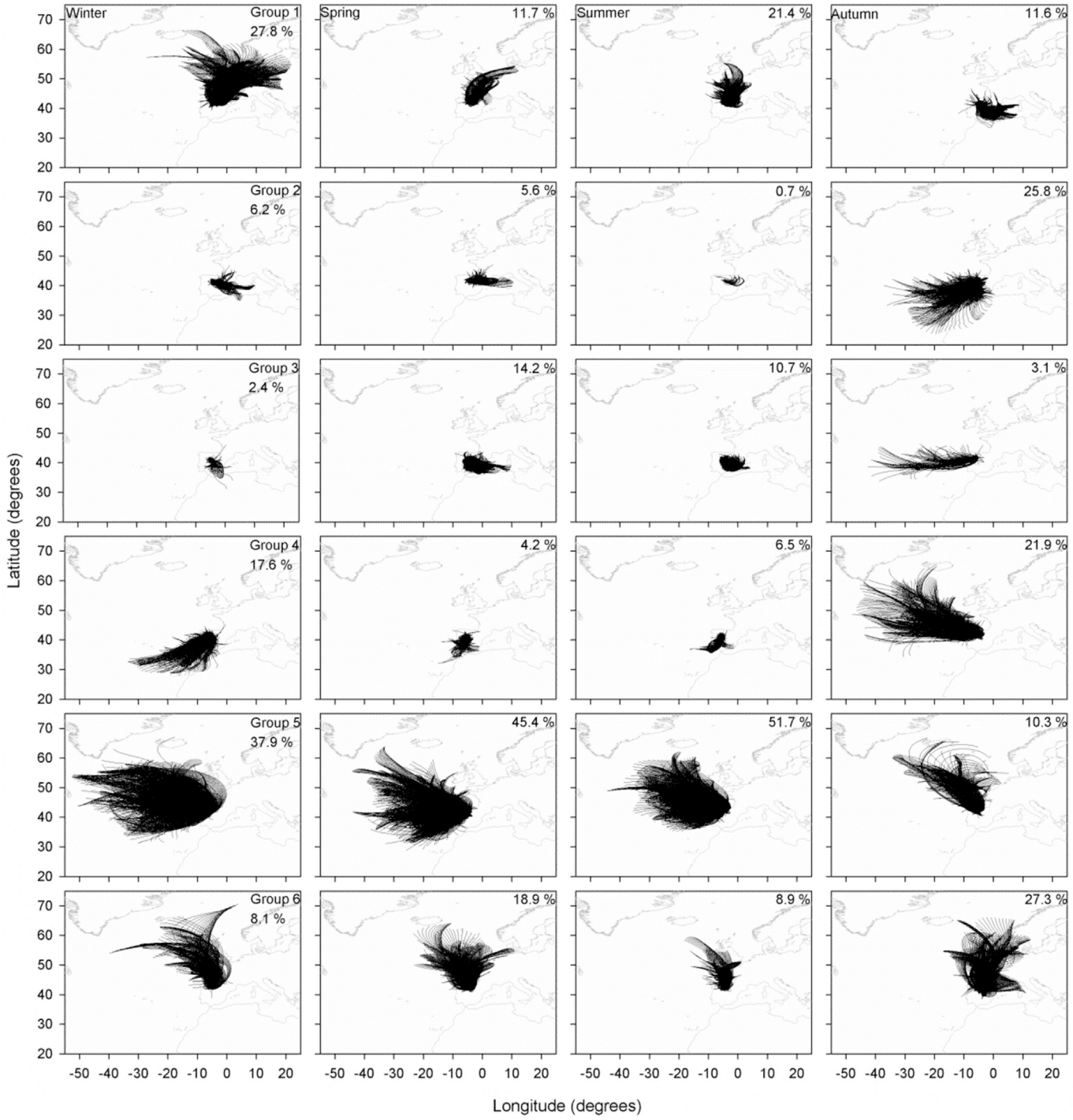


**Fig. 5.** Spaghetti plot of trajectories by season following the direction groups formed with the density of centroid directions. Each number corresponds to the seasonal frequency.

linked with continental air trajectories led to greater concentrations.

## 4. Discussion

### 4.1. Airflow description

The frequent zonal transport presented in Fig. 5 may be a consequence of the prevailing wind at this latitude and also of the geographical features. The western direction is free from orographic barriers, while the eastern direction presents a more complex topography and irregular land and sea surface distribution. Moreover, the link between the Icelandic Low and the North Atlantic Subtropical High conditioned the Atlantic flows. During the period analysed in this study, the North Atlantic Oscillation index was mainly negative, especially in summer, followed by autumn (NOAA, 2017), favouring westerly flows. An important consequence of this westerly transport was reported by Lozano et al. (2011) by means of the high activity concentrations of man-made radionuclides detected in the southwest Iberian Peninsula between March 28th and April 7th, 2011 due to the Fukushima nuclear power plant accident. Dueñas et al. (2011) also highlighted the influence of this kind of transport with similar plots when investigating the origin of air masses affecting the south of the peninsula and how these influence radionuclide

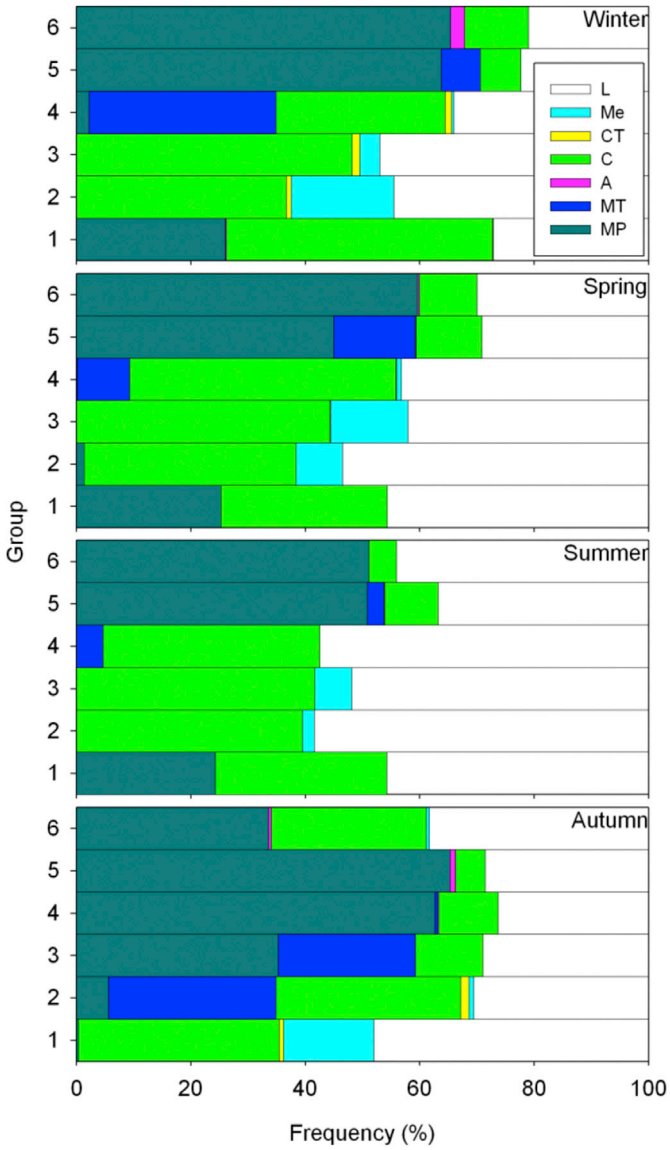


**Fig. 6.** Seasonal frequencies of the types of regions affecting the groups of trajectories.

**Table 1**
Mean seasonal concentration and standard deviation of $CO_2$ and $CH_4$ at the study site.

| Season | $CO_2$ (ppm) | | $CH_4$ (ppm) | |
|---|---|---|---|---|
| | Concentr. | Stand. dev. | Concentr. | Stand. dev. |
| Winter | 401.5 | 5.3 | 1.9174 | 0.0823 |
| Spring | 402.2 | 12.1 | 1.8951 | 0.0413 |
| Summer | 393.6 | 7.8 | 1.8789 | 0.0353 |
| Autumn | 399.5 | 8.0 | 1.9074 | 0.0837 |

activities.

The Mediterranean origin of air trajectories was less frequent than the Atlantic origin and might have been influenced by the negative phase of the Western Mediterranean Oscillation, which is associated with air masses from the Mediterranean Sea entering the Iberian Peninsula (Izquierdo et al., 2014).

Meridional transport is also affected by the distribution of pressure systems, since Roberge et al. (2009) reported significant precipitation along the west coast of North America due to transport from the tropical or subtropical Pacific Ocean. Trajectories from the south were very unusual. They have been observed in the south of the peninsula, where they led to desert dust intrusions (Negral et al., 2012; Valenzuela et al., 2012). However, these processes were infrequent in the north of the peninsula where high $PM_{10}$ concentrations (Cabello et al., 2012; Sánchez et al., 2007) or even red dust rain events were sometimes observed (White et al., 2012).

The features of the trajectory groups presented in Fig. 7 may be roughly classified using two possible procedures. One is the type of surface on which the air parcel is moving, and the second is the latitude of the departure site. Land surface is rougher than ocean surface, resulting in low speed and high altitude of air trajectories. Land surface is colder in winter than ocean surface and hotter in summer. Temperatures are lower for air trajectories from high latitudes than for air trajectories from low latitudes. Moreover, meteorological forcing and variations in the strength of the climatological pressure gradient exert a major influence.

In order to compare the resulting groups with previous analyses, cluster analyses of air parcel trajectories in the southern plateau gave similar mean trajectories, although the influence of the Mediterranean region was higher than that presented in this study, probably due to different orographic conditions in the two plateaus (Adame et al., 2012; Notario et al., 2013, 2014). These studies consider between three and five clusters, where the greatest contribution corresponded to the Atlantic Ocean, the northern direction origin being small, and the southern direction not appearing clearly. Pérez et al. (2015) analysed the airflow at the study site by five clusters where the highest extent was also reached in winter and the lowest in summer. Moreover, cluster distribution in autumn differed from the remaining seasons, in agreement with the pattern presented in Fig. 7.

### 4.2. *Influence of airflow on concentrations*

The concentrations presented in Table 1 are mainly controlled by soil and plant activities and also by atmospheric evolution. High $CO_2$ in spring, 402.2 ppm, was attributed to the decomposition of material from the previous autumn and winter together with intensive vegetation growth. These high $CO_2$ values are noticeable during the night, when stability prevails. However, the low value in summer, 393.6 ppm, was linked with the death of grass and crop harvest in this season (García et al., 2012). The $CH_4$ cycle reached its highest value in winter, 1.9174 ppm, and its lowest in summer, 1.8789 ppm, due to the photochemical reaction with OH radical in this period when solar radiation is intense and plant activity weakens (García et al., 2016; Sánchez et al., 2014). Moreover, the lowest boundary layer value was observed in winter, when stability is reinforced, and the highest in summer, when thermal turbulence is intensified since wind speed is low (Pérez et al., 2016). Consequently, dispersion and lower concentrations are favoured in summer.

Sreenivas et al. (2016) indicated that the marked negative correlation between wind speed and greenhouse gases was attributed to local sources, whereas poor correlation was linked to regional/local transport. These results were also observed at the study site, since short trajectories were obtained with low wind speeds and were associated with high concentrations. The absolute values of correlation coefficients calculated between distances travelled by average trajectories and concentrations shown in Fig. 7 were high, above 0.9 in autumn, confirming the strong influence of local sources in this season. These coefficients were intermediate, around 0.7, in winter and for $CO_2$ in summer, when local source influence is still important. Coefficients were low, below 0.5, in spring and for $CH_4$ in summer, when transport may also play a major role.

Another factor whose impact on the concentrations recorded should not be ignored involves nearby anthropogenic sources. This is the case of the city of Valladolid (around 300,000 people), located 24 km SE of the study site, and whose plume has been detected for high concentrations (Pérez et al., 2009). Moreover, $CH_4$ is affected not only by this city but also by a landfill located nearly 20 km from the study site in the same

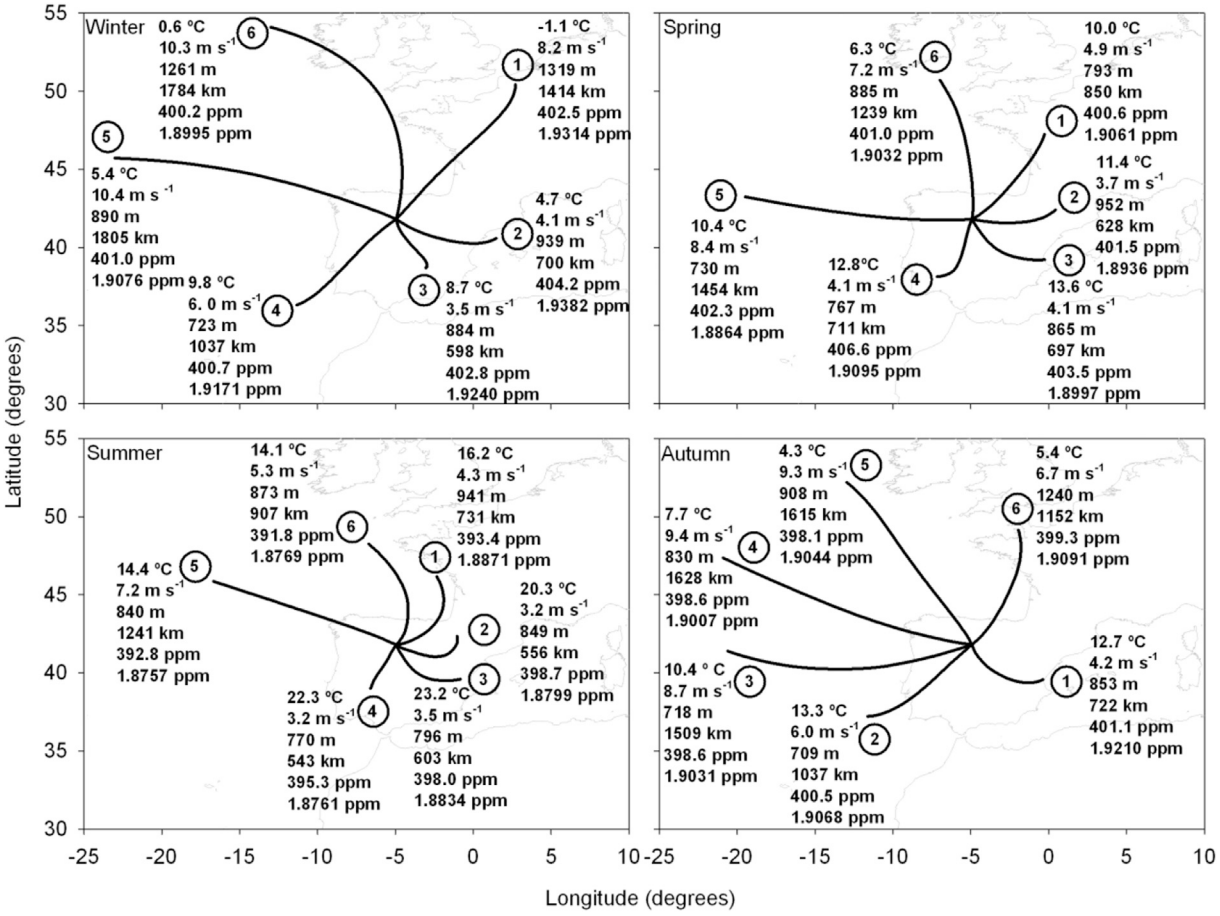


**Fig. 7.** Mean trajectories of the groups formed with their mean temperatures, wind speeds, heights above sea level, distances and $CO_2$ and $CH_4$ concentrations.

**Table 2**
Seasonal mean concentrations of merged groups, differences with mean seasonal value, and corresponding frequencies.

| Season | Groups | Freq. (%) | $CO_2$ (ppm) | $CO_2$ dif. (ppm) | $CH_4$ (ppm) | $CH_4$ dif. (ppm) |
|---|---|---|---|---|---|---|
| Winter | 1,2,3 | 35.9 | 402.8 | 1.3 | 1.9321 | 0.0147 |
| | 4,5,6 | 64.1 | 400.8 | −0.7 | 1.9091 | −0.0083 |
| Spring | 1,2,3,4 | 35.9 | 402.6 | 0.4 | 1.9020 | 0.0069 |
| | 5,6 | 64.1 | 401.9 | −0.3 | 1.8913 | −0.0038 |
| Summer | 2,3,4 | 18.8 | 396.9 | 3.3 | 1.8804[a] | 0.0015 |
| | 1,5,6 | 81.2 | 392.8 | −0.8 | 1.8786[a] | −0.0003 |
| Autumn | 1,6 | 38.7 | 399.8 | 0.3 | 1.9127 | 0.0053 |
| | 2,3,4,5 | 61.3 | 399.3 | −0.2 | 1.9040 | −0.0034 |

[a] The difference between these values is not statistically significant at a 95% confidence level.

direction as Valladolid (Sánchez et al., 2014). Consequently, air parcels from this direction might receive injections from both sources that may increase concentrations, although due to their proximity to the study site, the influence of these sources on each trajectory group may prove hard to establish.

This contrast between air trajectories of a different origin was observed at coastal sites on the peninsula where maritime transport scenarios are frequent, such as Lisbon with anthropogenic aerosols (Almeida et al., 2013). Another example can be found in Aveiro, with the organic compounds in rainwater (Santos et al., 2013). Lozano et al. (2012) used $^{7}Be$ and $^{210}Pb$ activities and observed differences between maritime and continental air trajectories reaching the south-western Iberian Peninsula to conclude that both radionuclides can be used as atmospheric transport markers. According to the results of the current analysis, $CO_2$ and $CH_4$ also mark the contrast between maritime and continental air trajectories within the peninsula. However, due to their close link with the ecosystem of the site, which determines their yearly evolution, their use as atmospheric transport markers requires further analysis.

## 5. Conclusions

A procedure to classify air parcel trajectories based on kernel density was proposed to obtain six groups of trajectories with marked directions, NNE-NE in winter, W in spring and WNW-NW in summer and autumn.

Inspection of trajectories revealed that zonal transport was more frequent than meridional transport. Moreover, air motion from the Atlantic Ocean was more frequent than trajectories from the Mediterranean Sea, and African trajectories were extremely infrequent compared to northern trajectories.

Geographical analysis of surface types below the air trajectories highlighted the influence of local features, particularly in summer. Atlantic influence was noticeable in autumn and the influence of mixed regions was observed in winter and spring.

Varied ranges were obtained in groups of winter trajectories, whereas ranges for summer trajectories were the shortest. The highest equilibrium between groups of maritime and continental air trajectories is observed in winter. This was lower in summer and both groups were not balanced in spring and autumn.

Stagnant conditions were responsible for higher concentrations of $CO_2$ and $CH_4$ than those observed for air trajectories from the Atlantic Ocean.

Finally, the procedure proposed in this study successfully classified air parcel trajectories more quickly than other firmly established

methods and may be a promising candidate for future analyses of this kind. Although density was calculated in this paper as a function of direction, the inclusion of additional variables, such as distance, in the study site may help to enhance our understanding and to provide fresh insights into air parcel trajectories, and is a line of research that merits further analysis. Moreover, future inquiry should also seek to offer a description of every group where the similarity of trajectories should be explored.

## Conflicts of interest

The authors declare there is no conflict of interests regarding publication of this paper.

## Acknowledgements

The authors wish to acknowledge the financial support of the Ministry of Economy and Competitiveness and ERDF funds (projects CGL2009-11979 and CGL2014-53948-P).

## References

Adame, J.A., Notario, A., Villanueva, F., Albaladejo, J., 2012. Application of cluster analysis to surface ozone, $NO_2$ and $SO_2$ daily patterns in an industrial area in Central-Southern Spain measured with a DOAS system. Sci. Total Environ. 429, 281–291.

Almeida, S.M., Silva, A.I., Freitas, M.C., Dzung, H.M., Caseiro, A., Pio, C.A., 2013. Impact of maritime air mass trajectories on the western european coast urban aerosol. J. Toxicol. Env. Heal. A 76, 252–262.

Buchholz, R.R., Paton-Walsh, C., Griffith, D.W.T., Kubistin, D., Caldow, C., Fisher, J.A., Deutscher, N.M., Kettlewell, G., Riggenbach, M., Macatangay, R., Krummel, P.B., Langenfelds, R.L., 2016. Source and meteorological influences on air quality (CO, $CH_4$ & $CO_2$) at a Southern Hemisphere urban site. Atmos. Environ. 126, 274–289.

Cabello, M., Orza, J.A.G., Barrero, M.A., Gordo, E., Berasaluce, A., Cantón, L., Dueñas, C., Fernández, M.C., Pérez, M., 2012. Spatial and temporal variation of the impact of an extreme Saharan dust event. J. Geophys. Res. 117, D11204 https://doi.org/10.1029/2012JD017513.

Cape, J.N., Methven, J., Hudson, L.E., 2000. The use of trajectory cluster analysis to interpret trace gas measurements at Mace Head, Ireland. Atmos. Environ. 34, 3651–3663.

Coury, C., Dillner, A.M., 2007. Trends and sources of particulate matter in the Superstition Wilderness using air trajectory and aerosol cluster analysis. Atmos. Environ. 41, 9309–9323.

Dimitriou, K., Kassomenos, P., 2013. The fine and coarse particulate matter at four major Mediterranean cities: local and regional sources. Theor. Appl. Climatol. 114, 375–391.

Dorling, S.R., Davies, T.D., Pierce, C.E., 1992. Cluster analysis: a technique for estimating the synoptic meteorological controls on air and precipitation chemistry-Method and applications. Atmos. Environ. A 26, 2575–2581.

Dueñas, C., Orza, J.A.G., Cabello, M., Fernández, M.C., Cañete, S., Pérez, M., Gordo, E., 2011. Air mass origin and its influence on radionuclide activities ($^{7}$Be and $^{210}$Pb) in aerosol particles at a coastal site in the western Mediterranean. Atmos. Res. 101, 205–214.

Fang, S.X., Tans, P.P., Dong, F., Zhou, H., Luan, T., 2016a. Characteristics of atmospheric $CO_2$ and $CH_4$ at the Shangdianzi regional background station in China. Atmos. Environ. 131, 1–8.

Fang, S., Tans, P.P., Steinbacher, M., Zhou, L., Luan, T., Li, Z., 2016b. Observation of atmospheric $CO_2$ and CO at Shangri-La station: results from the only regional station located at southwestern China. Tellus Ser. B-Chem. Phys. Meteorol. 68, 28506.

Fisher, N.I., 1993. Statistical Analysis of Circular Data. Cambridge University Press, Cambridge, UK, p. 277.

García, M.A., Sánchez, M.L., Pérez, I.A., 2012. Differences between carbon dioxide levels over suburban and rural sites in Northern Spain. Environ. Sci. Pollut. Res. 19, 432–439.

García, M.A., Sánchez, M.L., Pérez, I.A., Ozores, M.I., Pardo, N., 2016. Influence of atmospheric stability and transport on $CH_4$ concentrations in northern Spain. Sci. Total Environ. 550, 157–166.

Izquierdo, R., Alarcón, M., Aguillaume, L., Ávila, A., 2014. Effects of teleconnection patterns on the atmospheric routes, precipitation and deposition amounts in the north-eastern Iberian Peninsula. Atmos. Environ. 89, 482–490.

Kassomenos, P., Vardoulakis, S., Borge, R., Lumbreras, J., Papaloukas, C., Karakitsios, S., 2010. Comparison of statistical clustering techniques for the classification of modelled atmospheric trajectories. Theor. Appl. Climatol. 102, 1–12.

Li, M., Huang, X., Zhu, L., Li, J., Song, Y., Cai, X., Xie, S., 2012. Analysis of the transport pathways and potential sources of $PM_{10}$ in Shanghai based on three methods. Sci. Total Environ. 414, 525–534.

Lozano, R.L., Hernández-Ceballos, M.A., Adame, J.A., Casas-Ruíz, M., Sorribas, M., Miguel, E.G.S., Bolívar, J.P., 2011. Radioactive impact of Fukushima accident on the Iberian Peninsula: evolution and plume previous pathway. Environ. Int. 37, 1259–1264.

Lozano, R.L., Hernández-Ceballos, M.A., San Miguel, E.G., Adame, J.A., Bolívar, J.P., 2012. Meteorological factors influencing the $^{7}$Be and $^{210}$Pb concentrations in surface air from the southwestern Iberian Peninsula. Atmos. Environ. 63, 168–178.

Mahesh, P., Sreenivas, G., Rao, P.V.N., Dadhwal, V.K., Sai Krishna, S.V.S., Mallikarjun, K., 2015. High-precision surface-level $CO_2$ and $CH_4$ using off-axis integrated cavity output spectroscopy (OA-ICOS) over Shadnagar. India. Int. J. Remote Sens. 36, 5754–5765.

Markou, M.T., Kassomenos, P., 2010. Cluster analysis of five years of back trajectories arriving in Athens, Greece. Atmos. Res. 98, 438–457.

Negral, L., Moreno-Grau, S., Querol, X., Moreno, J., Viana, M., García-Sánchez, A., Alastuey, A., Moreno-Clavel, J., 2012. Weak pressure gradient over the Iberian Peninsula and African dust outbreaks: a new dust long-transport scenario. Bull. Am. Meteorol. Soc. 93, 1125–1132.

NOAA, 2017. North Atlantic Oscillation. http://www.cpc.ncep.noaa.gov/data/teledoc/nao.shtml. (Accessed 26 July 2017).

Notario, A., Adame, J.A., Bravo, I., Cuevas, C.A., Aranda, A., Díaz-de-Mera, Y., Rodríguez, A., 2014. Air pollution in the plateau of the Iberian peninsula. Atmos. Res. 145–146, 92–104.

Notario, A., Bravo, I., Adame, J.A., Díaz-de-Mera, Y., Aranda, A., Rodríguez, A., Rodríguez, D., 2013. Variability of oxidants ($OX=O_3+NO_2$), and preliminary study on ambient levels of ultrafine particles and VOCs, in an important ecological area in Spain. Atmos. Res. 128, 35–45.

Notaro, M., Alkolibi, F., Fadda, E., Bakhrjy, F., 2013. Trajectory analysis of Saudi Arabian dust storms. J. Geophys. Res. Atmos. 118, 6028–6043.

Pérez, I.A., Sánchez, M.L., García, M.A., de Torre, B., 2009. $CO_2$ transport by urban plumes in the upper Spanish plateau. Sci. Total Environ. 407, 4934–4938.

Pérez, I.A., Sánchez, M.L., García, M.A., Ozores, M., Pardo, N., 2014. Analysis of carbon dioxide concentration skewness at a rural site. Sci. Total Environ. 476–477, 158–164.

Pérez, I.A., Sánchez, M.L., García, M.A., Pardo, N., 2016. Features of the annual evolution of $CO_2$ and $CH_4$ in the atmosphere of a Mediterranean climate site studied using a nonparametric and a harmonic function. Atmos. Pollut. Res. 7, 1013–1021.

Pérez, I.A., Sánchez, M.L., García, M.A., Pardo, N., 2015. Analysis of air mass trajectories in the northern plateau of the Iberian Peninsula. J. Atmos. Sol.-Terr. Phys. 134, 9–21.

Pérez, I.A., Sánchez, M.L., García, M.A., Pardo, N., 2013. Carbon dioxide at an unpolluted site analysed with the smoothing kernel method and skewed distributions. Sci. Total Environ. 456–457, 239–245.

Roberge, A., Gyakum, J.R., Atallah, E.H., 2009. Analysis of intense poleward water vapor transports into high latitudes of western North America. Weather Forecast 24, 1732–1747.

Sánchez, M.L., García, M.A., Pérez, I.A., de Torre, B., 2007. Ground laser remote sensing measurements of a Saharan dust outbreak in Central Spain. Influence on $PM_{10}$ concentrations in the lower and upper Spanish plateaus. Chemosphere 67, 229–239.

Sánchez, M.L., García, M.A., Pérez, I.A., Pardo, N., 2014. $CH_4$ continuous measurements in the upper Spanish plateau. Environ. Monit. Assess. 186, 2823–2834.

Santos, P.S.M., Santos, E.B.H., Duarte, A.C., 2013. Seasonal and air mass trajectory effects on dissolved organic matter of bulk deposition at a coastal town in south-western Europe. Environ. Sci. Pollut. Res. 20, 227–237.

Snyder, J.P., 1987. Map Projections - a Working Manual. U.S. Government Printing Office, Washington, p. 383.

Sreenivas, G., Mahesh, P., Subin, J., Lakshmi Kanchana, A., Venkata Narasimha Rao, P., Kumar Dadhwal, V., 2016. Influence of meteorology and interrelationship with greenhouse gases ($CO_2$ and $CH_4$) at a suburban site of India. Atmos. Chem. Phys. 16, 3953–3967.

Tiwari, Y.K., Vellore, R.K., Ravi Kumar, K., van der Schoot, M., Cho, C.H., 2014. Influence of monsoons on atmospheric $CO_2$ spatial variability and ground-based monitoring over India. Sci. Total Environ. 490, 570–578.

Toledano, C., Cachorro, V.E., De Frutos, A.M., Torres, B., Berjón, A., Sorribas, M., Stone, R.S., 2009. Airmass classification and analysis of aerosol types at El Arenosillo (Spain). J. Appl. Meteorol. Climatol. 48, 962–981.

Valenzuela, A., Olmo, F.J., Lyamani, H., Antón, M., Quirantes, A., Alados-Arboledas, L., 2012. Classification of aerosol radiative properties during African desert dust intrusions over southeastern Spain by sector origins and cluster analysis. J. Geophys. Res. 117, D06214 https://doi.org/10.1029/2011JD016885.

White, J.R., Cerveny, R.S., Balling Jr., R.C., 2012. Seasonality in European red dust/"blood" rain events. Bull. Am. Meteorol. Soc. 93, 471–476.

Wilks, D.S., 2011. Statistical Methods in the Atmospheric Sciences. Academic Press, Amsterdam, p. 676.

Zeng, J., Matsunaga, T., Mukai, H., 2010. METEX - a flexible tool for air trajectory calculation. Environ. Modell. Softw. 25, 607–608.